

**Cavitation Phenomena and Performance of Oil  
Hydraulic Poppet Valve\***  
(5th Report, Influence of Dimensions of Valve  
on the Thrust Force Characteristics)

By Shigeru OSHIMA\*\* and Tsuneo ICHIKAWA\*\*\*

The thrust force characteristics of oil hydraulic poppet valves are studied experimentally. The thrust force is measured by using two apparatus; a half cut model and a full shaped model of a poppet valve, with the valve lift  $X$ , the seat chamfer length  $S$  and the poppet angle  $2\phi$  changed. The influence of the change in these three valve factors on the thrust characteristics is made clear by comparison of the thrust coefficients, and the mechanism of the change in the thrust characteristics is also made clear by studying the pressure distributions and the thrust force components within three different region along the poppet surface; the upstream region, the restricted part and the downstream region.

Key Words : Cavitation, Fluid Power Systems, Poppet Valve, Half Cut Model, Thrust Coefficient, Valve Lift, Chamfer Length, Poppet Angle, Experimental Study

### 1. Introduction

It is well-known that the dimensions and the form of a restricted part in an oil hydraulic poppet valve have a large effect on the characteristics of the valve. The effects of the valve lift, the seat chamfer length or the poppet angle on the discharge coefficients<sup>(1)-(3)</sup>, the thrust coefficients<sup>(4)-(6)</sup>, the valve stability<sup>(7)(8)</sup>, etc. have been investigated by many workers. However, there have been few works concerning the cavitation in a poppet valve. We know only the work by Aoyama and others<sup>(9)</sup>. Therefore, there remain many pending problems on a poppet valve performance accompanied by cavitation.

In the previous report<sup>(10)-(12)</sup>, we have clarified the influence of cavitation on the flow characteristics of a poppet valve with change of the valve lift, the seat chamfer length, the poppet angle and the oil temperature by using an original half cut model. Besides, the alteration of the thrust coefficients accompanied by cavitation occurrence has been studied and its mechanism has been revealed using some typical poppet valves in the last report<sup>(13)</sup>.

In this paper, for the purpose of understanding the influence of the size and the form of the restricted part in a poppet valve on the thrust performance accompanied by cavitation, an observation

of cavitation and a measurement of the pressure distributions are carried out in detail using a half cut model. The thrust coefficients are obtained by integrating the measured pressure distributions, and the effects of the valve dimensions on the thrust performance are investigated from the results. And the mechanism of the change in the thrust performance is revealed by studying the thrust force components within three different regions along the poppet surface; the upstream region, the restricted part and the downstream region.

### 2. The Experimental Method and the Arrangement of Result

The structure of the half cut model and the method of the measurement of pressure distribution have been presented in the first report<sup>(10)</sup> and the hydraulic circuit of the test apparatus in the second report<sup>(11)</sup>. The structure of the full shaped model designed the same as the half cut model has been shown in the fourth report<sup>(13)</sup>. The thrust force is directly measured using the load cell in the full shaped model. Comparing the results by the half cut model with those by the full shaped model, the agreement of the both results is confirmed. A quantitatively good agreement has been confirmed between the thrust coefficients in the both results concerning several typical poppet valves in the fourth report<sup>(13)</sup>.

The important dimensions of the half cut model and the full shaped model used in this experimentation are given in Table 1.  $S$  is the chamfer length of the valve seat, and the vertical angle of the tapered surface of the chamfer is the same as the poppet angle  $2\phi$  in every case. The oil temperature is held at  $40 \pm 1^\circ\text{C}$ , the

\* Received 22nd November, 1984.

\*\* Assistant Professor, Numazu College of Technology (3600 Ooka, Numazu, Shizuoka, Japan)

\*\*\* Professor, Toyohashi University of Technology (1-1 Hibarigaoka, Tenpaku-cho, Toyohashi, Aichi, Japan)

density  $\rho=851 \text{ kg/m}^3$  and viscosity  $\mu=4.6 \times 10^{-2} \text{ Pa}\cdot\text{s}$ .

In the arrangement of the results, the thrust coefficients are defined by the same method as in the fourth report<sup>(13)</sup>.  $C_{FP}$  is the thrust coefficient obtained by integrating the pressure distribution along the poppet surface in the half cut model and  $C_{FL}$  is the one obtained by the direct measurement with the full shaped model.

In this paper, the difference of the curves of  $C_{FP}$  or  $C_{FL}$  is studied changing the valve lift  $X$ , the seat chamfer length  $S$  and the poppet angle  $2\phi$ , with the increase of the pressure difference  $\Delta P (=P_1 - P_2)$  with the upstream pressure  $P_1$  fixed at 5 MPa(abs.). Besides, for the purpose of understanding the mechanism of the alteration in the thrust coefficient, the thrust components are obtained respectively within the three divided regions\* as shown in Fig.1; the upstream region, the restricted part and the downstream region. The thrust force components are obtained by integrating the pressure distributions along the poppet surface within each region. The non-dimensional differential thrust components  $\overline{\Delta F_1}$ ,  $\overline{\Delta F_2}$ ,  $\overline{\Delta F_3}$  are obtained by dividing the difference between the thrust components with  $X=0 \text{ mm}$  and  $X=(\text{positive}) \text{ mm}$  by  $F_{\text{max}}$  which is the thrust force all over the poppet surface when  $P_2$  is equal to  $P_1$ . They are defined by Eq.(1) for the diverging flow and Eq.(2) the converging flow.  $F_{\text{max}}$  is obtained by Eq.(3). (diverging flow)

$$\begin{aligned} \overline{\Delta F_1} &= \left( \int_{A_1} P_p dA - P_1 A_1 \right) / F_{\text{max}} \\ \overline{\Delta F_2} &= \left( \int_{A_1} P_p dA - \frac{P_1 + P_2}{2} A_2 \right) / F_{\text{max}} \\ \overline{\Delta F_3} &= \left( \int_{A_3} P_p dA - P_2 A_3 \right) / F_{\text{max}} \end{aligned} \quad \dots\dots\dots(1)$$

(converging flow)

$$\overline{\Delta F_1} = \left( \int_{A_3} P_p dA - P_1 A_3 \right) / F_{\text{max}}$$

$$\begin{aligned} \overline{\Delta F_2} &= \left( \int_{A_2} P_p dA - \frac{P_1 + P_2}{2} A_2 \right) / F_{\text{max}} \\ \overline{\Delta F_3} &= \left( \int_{A_1} P_p dA - P_2 A_1 \right) / F_{\text{max}} \end{aligned} \quad \dots\dots\dots(2)$$

$$F_{\text{max}} = P_1 (A_1 + A_2 + A_3) \quad \dots\dots\dots(3)$$

where,  $P_1$  is the upstream pressure,  $P_2$  the downstream pressure and  $P_p$  the pressure along the poppet surface, of which typical curves are shown in Fig.1. The actual measured results of  $P_p$  are shown in the fourth report<sup>(13)</sup>.  $A_1$ ,  $A_2$  and  $A_3$  are the areas of the three divided regions on the poppet cone surface as projected on to the plane which is perpendicular to the central axis. In the case of the diverging flow,  $A_1$  is the upstream region,  $A_2$  the restricted part and  $A_3$  the downstream region. In the case of the converging flow,  $A_1$  is the downstream region,  $A_2$  the restricted part and  $A_3$  the upstream region.

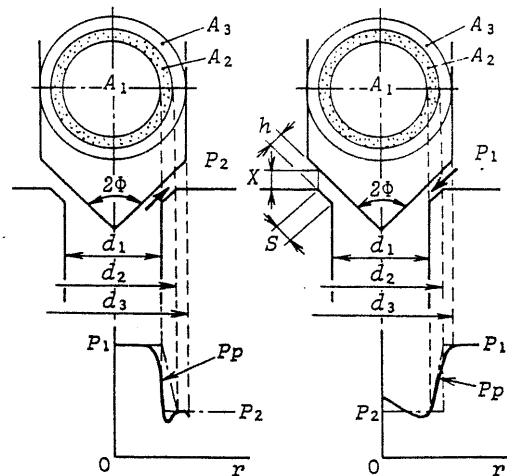
3. Influence of the valve lift

Figure 2 shows the thrust coefficient  $C_{FL}$  with  $X=0.2 \text{ mm}$  and  $0.4 \text{ mm}$ , in the case of the full shaped model with the seat NO.3. The upper drawing shows the result of the diverging flow and the lower the converging flow. The mark  $\curvearrowright$  indicates an inception of cavitation. On the other hand, Figs.3 and 4 show the thrust coefficient  $C_{FP}$  and the non-dimensional differential thrust components  $\overline{\Delta F_1}$ ,  $\overline{\Delta F_2}$ ,  $\overline{\Delta F_3}$  with  $X=0.4 \text{ mm}$  and  $0.8 \text{ mm}$  in the case of the half cut model with the seat NO.3. The mark  $\curvearrowright$  indicates an inception and  $\curvearrowleft$  does a cavitation occurrence at the entrance corner of the restriction. They show the results when  $P_2$  is reduced with  $P_1$  fixed at 5 MPa(abs.). Comparing  $C_{FP}$  with  $C_{FL}$ , it can be confirmed that the influence of  $X$  on the thrust performance

Table 1 Important dimensions of the test valves

Seat NO.	S mm	d <sub>1</sub> mm	d <sub>2</sub> mm	d <sub>3</sub> mm	2φ°
Full Model	1	0	12.10	—	90
	2	0.64	12.02	12.93	
	3	1.35	12.04	13.95	
	4	2.27	12.05	15.26	
	6	1.16	12.08	13.23	
Half Cut Model	1	0	12.00	—	18.00
	2	0.65	12.00	12.92	18.00
	3	1.32	12.01	13.87	
	4	2.32	12.05	15.33	
	6	1.25	11.99	13.24	18.00
9	1.17	11.99	12.88	18.00	45

\* 90°, 60° and 45°



(a) Diverging flow (b) Converging flow

Fig.1 The divided regions for the calculation of the thrust components

\*1 The two divided regions in the case of the non-chamfered valve

has the same tendency in both the full shaped model and the half cut model.

In the case of the diverging flow,  $C_{Fl}$  and  $C_{Fp}$  become small with an increase of  $X$  because the flow rate increases and the pressure reduction becomes larger in the upstream region. This is understood from the reduction of  $\overline{\Delta F_1}$  in Fig.3.

In the case of  $X=0.4$  mm in Figs.2 and 3, the curves of the thrust coefficient show especially a clear change accompanied by the occurrence of cavitation. The reason is explained as follows. The occurrence of cavitation at the entrance of the restriction induces a large pressure reduction in the restricted part and the pressure drops below  $P_2^{(13)}$ , so that  $\overline{\Delta F_2}$  decreases sharply and the thrust coefficient decreases. Then, when the flow saturates to a constant value<sup>(10)</sup> with an increase of  $\Delta P$ , the pressure distribution within the upstream region does not change, and  $\overline{\Delta F_1}$  becomes therefore constant. Hence, the slope of the thrust coefficient becomes mild again. When  $X$  is less than 0.4 mm, this change in the thrust coefficient is not clear because the cavitation does not occur for small  $\Delta P$ , and when  $X$  is larger than 0.4 mm, the flow saturation is not clear because the ratio  $S/h$  is small and the valve characteristics approach those of the valve with a small chamfer length.

In the converging flow, the thrust coefficient becomes large as  $X$  is larger unlike in the diverging flow. This result is due to the increase of  $\overline{\Delta F_2}$  induced by the pressure rise near the entrance of the restriction and to the increase of  $\overline{\Delta F_3}$  induced by the dynamic pressure caused by the concentration and bend of jet in the downstream region<sup>(13)</sup>.  $\overline{\Delta F_1}$  decreases as  $X$  becomes larger because the pressure reduction becomes large in the upstream region in the same manner as the diverging flow, but the degree of its reduction is less than the increase of  $\overline{\Delta F_2}$  and  $\overline{\Delta F_3}$ . Hence, the thrust coefficient becomes larger as  $X$  is larger.

From Fig.4, it is understood that  $C_{Fp}$  decreases discontinuously with the cavitation occurrence at the entrance in the case of  $X=0.8$  mm. This is due to the alteration of  $\overline{\Delta F_3}$  induced by the change of the pressure distribution in the downstream region.

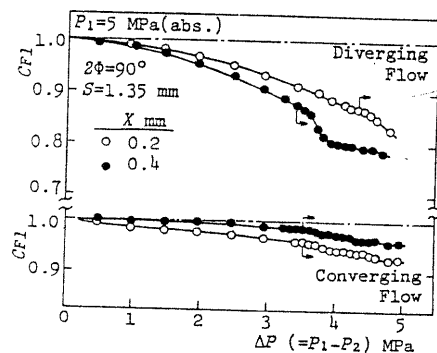


Fig.2 Influence of the valve lift (Full shaped model)

Comparing the cases of the diverging flow and the converging flow, the change of the thrust coefficient with  $X$  is not so clear in the converging flow. This is considered to come from the fact that the alteration of  $\overline{\Delta F_1}$  offsets the alteration of  $\overline{\Delta F_2}$  and  $\overline{\Delta F_3}$  with the change of  $X$  in the converging flow.

#### 4. Influence of the Chamfer Length

Figure 5 shows  $C_{Fl}$  with a changing chamfer length  $S$  with  $X=0.4$  mm and  $2\phi=90^\circ$ . The upper drawing shows the diverging flow and the lower the converging flow. Figures 6 and 7 show  $C_{Fp}$ ,  $\overline{\Delta F_1}$ ,  $\overline{\Delta F_2}$  and  $\overline{\Delta F_3}$  with change of  $S$  with  $X=0.8$  mm and  $2\phi=90^\circ$  in the case of the half cut model. As the valve characteristics depend on the ratio  $S/h$ <sup>(11)</sup>, the parameter is described with  $S/h$ . It is confirmed that  $C_{Fl}$  and  $C_{Fp}$  show the same tendency with the change of  $S/h$ . In the case of the diverging flow,

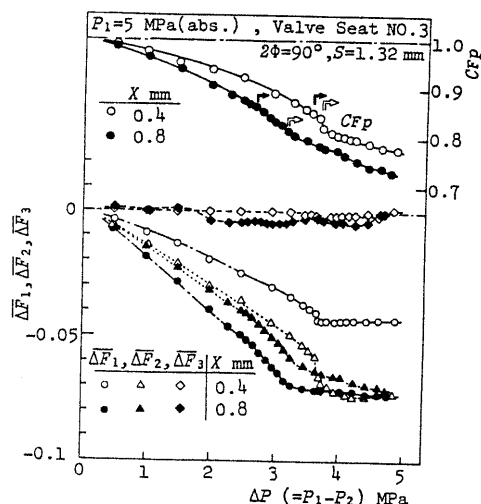


Fig.3 Influence of the valve lift (Half cut model, Diverging flow)

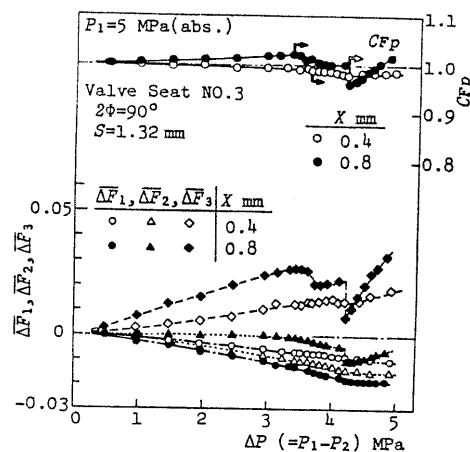


Fig.4 Influence of the valve lift (Half cut model, Converging flow)

the thrust coefficient becomes small and the change of it with the cavitation occurrence becomes clearer as  $S/h$  is larger. This result is explained as follows. The pressure reduction becomes large in the restricted part when a cavitation occurs at the entrance and the projection area of the restricted part becomes larger as  $S/h$  is larger with a fixed  $X$ . Hence,  $\overline{\Delta F_2}$  decreases greatly with the cavitation occurrence. And the flow saturation appears more clearly as  $S/h$  is larger<sup>(11)</sup>, so that  $\overline{\Delta F_1}$  becomes constant with higher accuracy under the cavitating condition.

A little increase of  $C_{FP}$  happens with the cavitation occurrence in the cases of

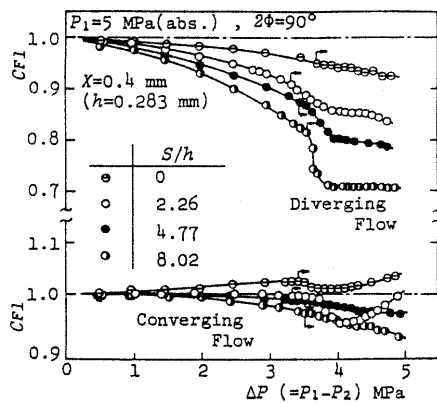


Fig.5 Influence of the chamfer length (Full shaped model)

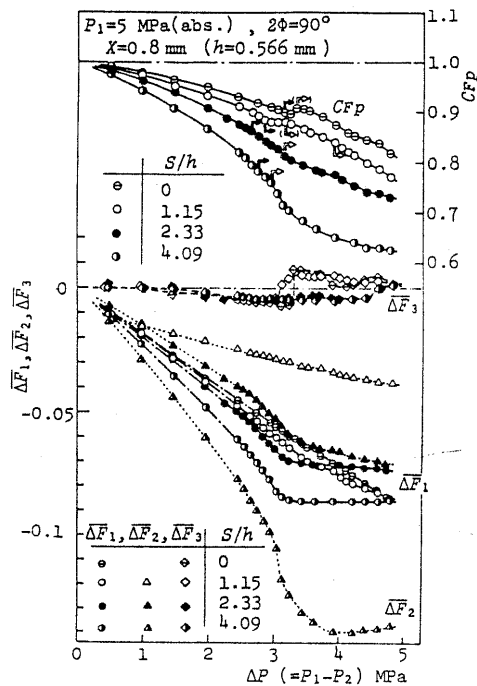


Fig.6 Influence of the chamfer length (Half cut model, Diverging flow)

$S/h=0$  and 1.15. This phenomenon is due to the change of  $\overline{\Delta F_1}$  induced by the alteration of the downstream pressure distribution. This will be examined in detail in the next section.

In the case of the converging flow, it is understood from Figs.5 and 7 that the thrust coefficient becomes larger than unity when  $S/h=0$ , but it becomes close to or less than unity when the seat has a chamfer. This is caused by  $\overline{\Delta F_1}$  becoming small and  $\overline{\Delta F_2}$  becoming negative in the case of a chamfered valve.

When  $S/h$  is small, a sudden reduction appears in the thrust coefficient in Fig.7. Especially in the case of  $S/h=1.15$ ,  $C_{FP}$  drops discontinuously and greatly. This is mainly due to the sudden change of  $\overline{\Delta F_1}$  induced by the change of the pressure distribution in the downstream region<sup>(11)</sup>.

Generally,  $\overline{\Delta F_1}$  becomes large,  $\overline{\Delta F_2}$  small and  $\overline{\Delta F_3}$  does not change with an increase of  $S/h$  in the non-cavitating region, except in the case of  $S/h=0$ . Hence, there is little difference in the thrust coefficients with the change of  $S/h$  in the non-cavitating region of the three cases.

### 5. Influence of the Poppet Angle

Figure 8 shows the alteration of  $C_{FI}$  with change of the poppet angle  $2\phi$ . In this case, the valve lift is so set that the clearance height  $h$  of the restriction becomes equal to 0.283 mm. The upper drawing shows the diverging flow and the lower the converging flow. Figures 9 and 10 show the result by the half cut model with three different values of  $2\phi$  and  $h$  fixed at 0.566 mm. Figure 9 shows the diverging flow and Fig.10 the converging flow.

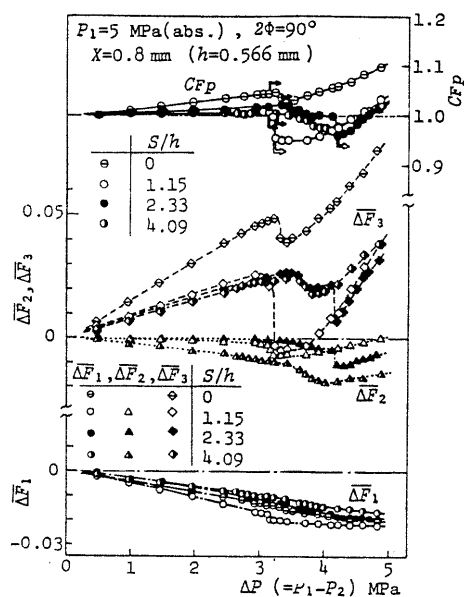


Fig.7 Influence of the chamfer length (Half cut model, Converging flow)

In the case of the diverging flow, it is understood from the results of  $C_{F1}$  and  $C_{FP}$  that the thrust coefficient becomes small and the change of it with the cavitation occurrence happens more clearly as  $2\phi$  is larger. This is due to the reduction of  $\Delta F_2$  with an increase of  $2\phi$ . The flow bend angle becomes sharper, the separation and the concentration of the stream line become stronger near the entrance of the restriction, which induces a large pressure reduction in the restricted part. Besides, the projection area of the restricted part becomes larger with an increase of  $2\phi$ . Since the flow passage area in the upstream region is larger as  $2\phi$  is larger for the same distance from the restriction, the pressure reduction becomes small, so that  $\Delta F_1$  becomes larger as  $2\phi$  is larger. However, since the degree of reduction of  $\Delta F_2$  is greater than the increase of  $\Delta F_1$ , the result mentioned above happens. It is considered therefore that the results in Figs.8 and 9 depend on

the chamfer length  $S$  strongly and become clearer when  $S$  becomes larger.

In the converging flow, the discontinuous reduction of the thrust coefficient with the cavitation occurrence at the entrance happens more clearly as  $2\phi$  is smaller. This is explained as follows. The flow bend angle becomes sharper and the separation and concentration of the stream line become stronger near the entrance of the restriction as  $2\phi$  is smaller. Therefore, the cavitation occurs suddenly at the entrance, which induces a large pressure reduction in the restricted part and the downstream region<sup>(12)</sup>. This can be known from the changes of  $\Delta F_2$  and  $\Delta F_3$  in Fig.10.

$\Delta F_3$  becomes larger as  $2\phi$  is larger, because the pressure is higher near the outlet of the restriction and the dynamic pressure induced by the bend and the concentration of the jet becomes larger in the downstream region.

On the other hand,  $\Delta F_1$  and  $\Delta F_2$  become smaller as  $2\phi$  is larger. This can be understood easily by Bernoulli's theorem. Since the changes of  $\Delta F_1$  and  $\Delta F_2$  offset the change of  $\Delta F_3$  with the alteration of  $2\phi$ , there is not a clear difference in the thrust coefficients in the non-cavitating region in Fig.10.

Figure 11 shows the result by the half cut model with three different values of  $2\phi$  and  $S=0$  mm in the case of the diverging flow. The non-dimensional differential thrust components are described with  $\Delta F_1$  in the upstream region and with  $\Delta F_3$  in the downstream region. There is not a component of  $\Delta F_2$  because of  $S=0$  mm. The valve lift is so set that  $h$  may be 0.566 mm in the same manner as in Fig.9.

It is understood that the thrust coefficient becomes smaller as  $2\phi$  is

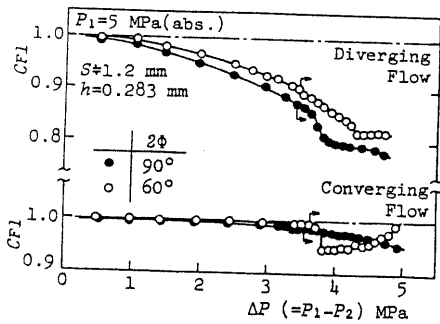


Fig.8 Influence of the poppet angle (Full shaped model)

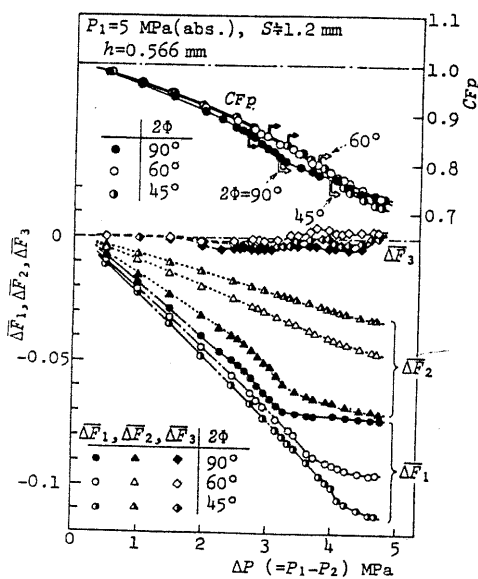


Fig.9 Influence of the poppet angle (Half cut model, Diverging flow,  $S=1.2$  mm)

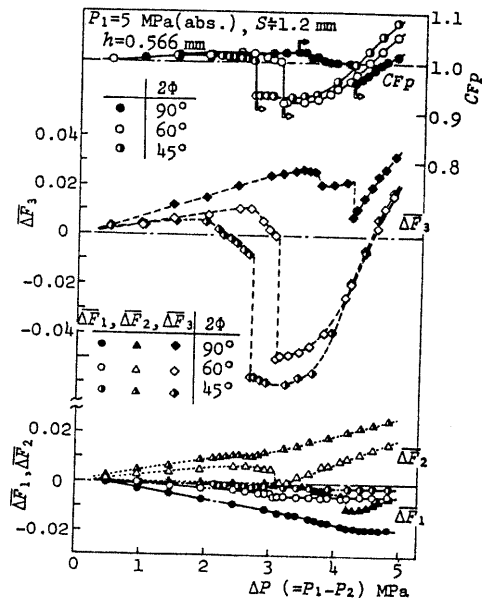


Fig.10 Influence of the poppet angle (Half cut model, Converging flow,  $S=1.2$  mm)

smaller unlike the result in Fig.9. This is due to the reduction of  $\overline{\Delta F_1}$  induced by the increase of the pressure drop in the upstream region. There is little difference in  $\overline{\Delta F_1}$  with the change of  $2\phi$ .

It can be known from Fig.11 that  $C_{FP}$  increases temporarily with the cavitation occurrence, as mentioned in the previous section. It is understood from the result of Fig.11 that this phenomenon is due to the change of  $\overline{\Delta F_3}$  caused by the alteration of the pressure distribution with the change of the flow pattern near the corner on the poppet surface in the downstream region. Figure 12 shows the alteration of the pressure at the point (B) which is 0.2 mm distant from the corner (A), and sketches of the condition of cavitation are given together. Besides, Fig.13 shows the change of the pressure distribution near the corner (A).

According to the observation, it is known that there are two different flow conditions with the change of  $\Delta P$ ; in one condition the flow changes its direction at (A) and reattaches itself to the surface of the poppet shank as shown in the region of (III) in Fig.12, in the other the flow goes on without reattachment as shown (II) and (IV). It is known from Fig.13 that the pressure drops sharply near the corner (A) when the flow pattern is (III), but when it is (II) or (IV) the pressure does not drop so sharply near (A) but rises above  $P_2$  in a specified region upstream of (A). In the region (I), though the flow pattern is not able to be observed because of no cavitation, it is considered similar to that in (III) by comparison of the pressure distributions in Fig.13. Hence, it seems that the temporal increase of the thrust coefficient in Fig.11 is caused by the alteration of the pressure distribution along the poppet surface with the change of the flow

pattern from (I) to (II). There is a little alteration in the thrust coefficient also with the changes of the flow pattern from (II) to (III) and (III) to (IV). There is hysteresis in the changes of (II) to (III) and (III) to (IV), but none in the change of (I) to (II).

When the valve seat has a large chamfer, the changes of the flow pattern from (I) to (II) and (II) to (III) do not occur clearly. It is considered that the flow pattern is (III) even in the incipient cavitation condition in this case.

Figure 14 shows a case of the converging flow with  $S=0$  mm. It is understood from this result that the thrust coefficient becomes larger as  $2\phi$  is smaller generally, being induced by the increase of  $\overline{\Delta F_1}$ . In the case of  $2\phi=45^\circ$ , the pressure is considered almost equal to  $P_1$  in the upstream region because of  $\overline{\Delta F_1} \approx 0$ .

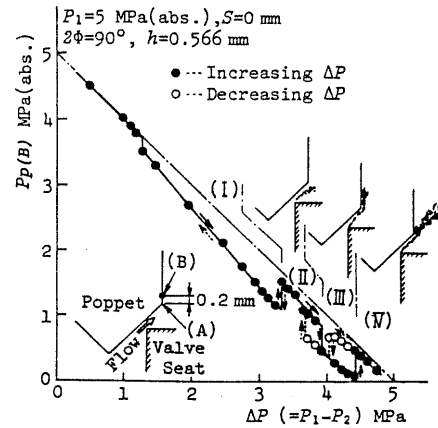


Fig.12 Alteration of the pressure at the point (B) (Diverging flow,  $2\phi=90^\circ$ ,  $S=0$  mm)

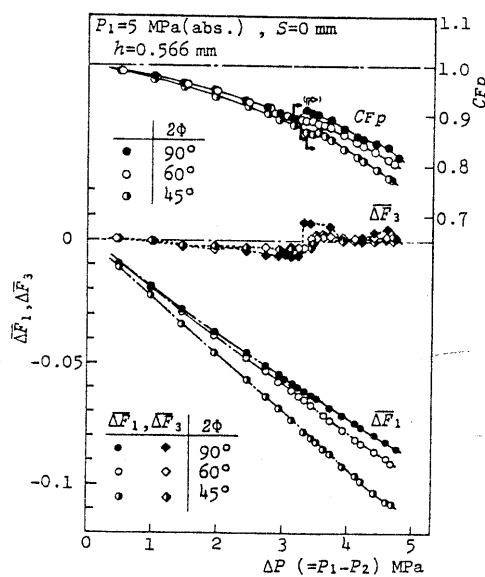


Fig.11 Influence of the poppet angle (Half cut model, Diverging flow,  $S=0$  mm)

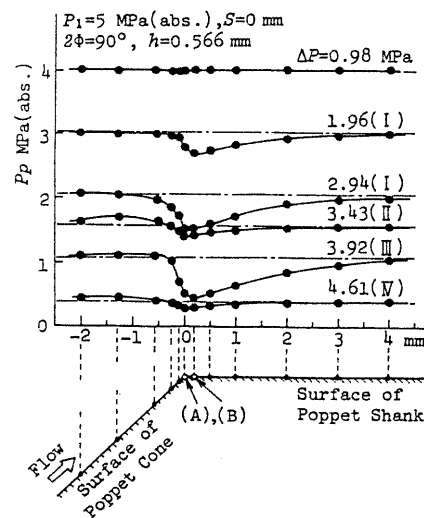


Fig.13 Alteration of the pressure distribution along the poppet surface in the downstream region (Diverging flow,  $2\phi=90^\circ$ ,  $S=0$  mm)

The alteration of the thrust coefficient with the cavitation occurrence is clearer as  $2\phi$  is smaller. This alteration is due to the change of  $\Delta F_3$ .

6. Conclusions

The influence of the important dimensions of an oil hydraulic poppet valve on the thrust force characteristics accompanied by cavitation is made clear by experimentations with the half cut model and the full shaped model, changing the valve lift, the seat chamfer length and the poppet angle. Also, the mechanism of the change of the thrust performance is revealed by detailed examinations of the pressure distributions along the poppet surface. The important results are as follows.

(1) The thrust coefficient becomes smaller as the valve lift is larger when the valve seat has a chamfer in the case of a diverging flow.

The thrust coefficient decreases sharply with the cavitation occurrence at the entrance of the restriction. This is mainly due to the reduction of the pressure in the restricted part. This change occurs most clearly with a specified valve lift.

(2) In the case of a converging flow, the thrust coefficient becomes larger as the valve lift is larger unlike the result (1). This is mainly due to the dynamic pressure caused by the bend and the concentration of a jet in the downstream region. The difference of the thrust coefficients with the change of  $X$  is less wide than in the diverging flow.

(3) The thrust coefficient becomes small and the alteration with the cavitation occurrence becomes clearer as  $S/h$  is larger in the case of a diverging flow. This is due to the increase of the pressure reduction and the projection area of

the restricted part with an increase of  $S/h$ .

(4) In the case of a converging flow, the thrust coefficient becomes larger than unity when  $S/h=0$ , but it becomes close to or less than unity when the seat has a chamfer. This is mainly due to  $\Delta F_3$  becoming negative by the pressure reduction in the restricted part.

The thrust coefficient drops discontinuously with the cavitation occurrence at the entrance of the restriction when  $S/h$  is small. This is due to a sudden change of the pressure distribution in the downstream region.

(5) The thrust coefficient becomes smaller as  $2\phi$  is larger unlike the result of  $S=0$  mm in the case of a diverging flow. This is due to an increase in the pressure reduction and in the projection area of the restricted part with an increase of  $2\phi$ .

(6) In a converging flow, the discontinuous reduction of the thrust coefficient occurs more clearly with the cavitation occurrence at the entrance of the restriction as  $2\phi$  is smaller.

$\Delta F_3$  becomes larger as  $2\phi$  is larger because the pressure rise by the bend and the concentration of the jet becomes larger in the downstream region.

(7) When  $S$  is zero or considerably small, the flow pattern and the pressure distribution suddenly change with  $\Delta P$  near the corner produced by the poppet cone surface and the shank. It causes a little temporal rise in the thrust coefficient.

The authors wish to thank Mr. Hibi in Toyohashi University of Technology for his useful advice.

References

- (1) Takenaka, T. and Urata, E., Trans. Jpn. Soc. Mech. Eng. (in Japanese), Vol. 33, No. 249 (1967-5), p. 810.
- (2) Kasai, K., Trans. Jpn. Soc. Mech. Eng. (in Japanese), Vol. 33, No. 251 (1967-7), p. 1083.
- (3) Kato, T., et al., Trans. Jpn. Soc. Mech. Eng. (in Japanese), Vol. 48, No. 427, B (1982-3), p. 581.
- (4) Stone, J. A., Trans. ASME, Ser. D., Vol. 82, No. 1 (1960-3), p. 144.
- (5) Urata, E., Trans. Jpn. Soc. Mech. Eng. (in Japanese), Vol. 35, No. 270 (1969-2), p. 358.
- (6) Scheffel, G., Öl. u. Pneu., 21, Nr. 8 (1977), p. 551.
- (7) Kojima, E., Trans. Jpn. Soc. Mech. Eng. (in Japanese), Vol. 38, No. 310 (1972-6), p. 1437.
- (8) Maeda, T., Trans. Jpn. Soc. Mech. Eng. (in Japanese), Vol. 35, No. 274 (1969-6), p. 1285.
- (9) Aoyama, Y., et al., J. Hy. & Pneu. (in Japanese), Vol. 11, No. 4 (1980-7), p. 246.
- (10) Oshima, S. and Ichikawa, T., Trans. Jpn. Soc. Mech. Eng. (in Japanese), Vol. 51, No. 462, B (1985-2), p. 427.
- (11) Oshima, S. and Ichikawa, T., Trans. Jpn. Soc. Mech. Eng. (in Japanese), Vol. 51, No. 462, B (1985-2), p. 628.
- (12) Oshima, S. and Ichikawa, T., Trans. Jpn. Soc. Mech. Eng. (in Japanese), Vol. 51, No. 467, B (1985-7), p. 2043.
- (13) Oshima, S. and Ichikawa, T., Trans. Jpn. Soc. Mech. Eng. (in Japanese), Vol. 51, No. 467, B (1985-7), p. 2249.

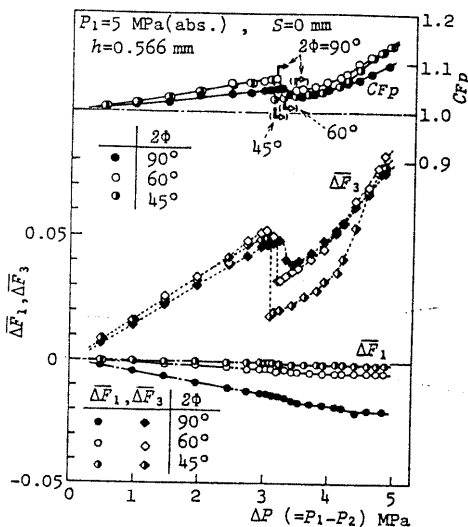


Fig. 14 Influence of the poppet angle (Half cut model, Converging flow,  $S=0$  mm)